JOINT INSTITUTE FOR NUCLEAR RESEARCH
Bogoliubov Laboratory of Theoretical Physics

FINAL REPORT ON THE START PROGRAMME

Parton polarization effects of Drell-Yan process

Supervisor:
Dr. Alexey Zhevlakov

Student:
Iurii Anikin, Russia
Tomsk State University

Participation period:
August 13 – September 23,
Summer Session 2023

Dubna, 2023

ABSTRACT

Parton polarization effects are one of the most efficient tools for investigation of the structure of hadrons.

Direct calculations reveal that to achieve precise descriptions of experimental data, it is necessary to consider at least the first-order corrections with respect to the strong interaction constant α_s. Therefore, the goal of this work is to obtain the helicity structure functions for the polarized Drell-Yan process at the first order of the strong coupling constant α_s.

We developed Wolfram Mathematica program code for helicity structure functions analytical calculation. Through this code usage, we got expressions for helicity structure functions in polarized initial partons case of Drell-Yan process. It turned out that taking into account the polarization of the initial partons led to the appearance of two new structure functions W_{T_P} and W_{∇_P} compared to the unpolarized case.

CONTENTS

INTRODUCTION

The quest for unraveling the most fundamental constituents of matter has reached a pivotal juncture, culminating in the establishment of the Standard Model of particle physics, a framework whose foundations were laid down in the 1970s. This comprehensive model not only categorizes all known elementary particles but also delineates the intricate interplay of their interactions through the bedrock forces of electromagnetism, the strong nuclear force, and the weak nuclear force. Undeniably, the Standard Model has triumphed in predicting the existence and properties of particles, including the remarkable W and Z bosons, and its empirical confirmation has been achieved with remarkable precision.

Nonetheless, the Standard Model's scope is not all-encompassing; it finds itself unable to elucidate certain perplexing phenomena, notably the origins of neutrino masses and the enigmatic nature of dark matter. In response to these unresolved mysteries and in pursuit of stringent tests for the Standard Model, the construction of the Large Hadron Collider (LHC) was undertaken. This colossal scientific apparatus, with its unparalleled collision energies involving protons, seeks to probe the deepest recesses of the subatomic realm. However, to wield the LHC as a precision instrument in this scientific quest, an intricate comprehension of the proton, one of its central constituents, is imperative. This thesis focuses on the theoretical treatment of one of the processes, which provides essential information on the structure of the proton, the Drell-Yan process [2]:

$$h(P_A) + h'(P_B) \to V(q) + X \to l_- + l_+ + X, \tag{1}$$

where P_A и P_B — beam and target momenta;

l_+ и l_- — lepton momenta;

$q = l_+ + l_-$ — boson momentum.

where two hadrons are collided to form a lepton-antilepton pair and additional debris particles X, which are usually of less interest then the lepton pair.

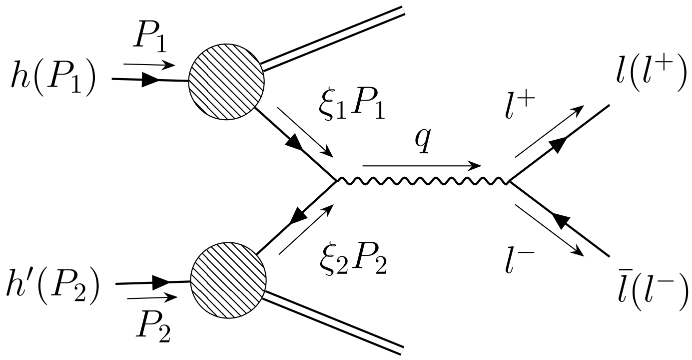

Figure 1: Drell-Yan process in zero order of α_s

Today, the Drell-Yan process remains a fundamental method for examining the inner composition of hadrons. Even with the present high energy level of 14 TeV at the LHC, it allows us to discern the influences of more massive quark types like strange or charm. As a result, it offers an avenue to refine our understanding of the proton's inner structure, a critical aspect for uncovering novel phenomena and achieving precise measurements in all contemporary and forthcoming hadron-hadron colliders.

1 Drell-Yan process basics

1.1 Kinematics

In order to describe the Drell-Yan process we will use two coordinate frames: the hadron c.m.s and the dilepton c.m.s. .

1.1.1 Hadron center-of-mass system

Let us choose the z-axis direction along beam direction. And the x-axis — along transverse momentum of the photon.

$$\vec{q}_T = \begin{pmatrix} Q_x \\ Q_y \\ 0 \end{pmatrix}. \tag{2}$$

On the other hand, the y-axis just follows from the right hand rule. Therefore, kinematics variables in hadron c.m.s have the following form:

$$P_A = \frac{1}{2}\begin{pmatrix} \sqrt{s} \\ 0 \\ 0 \\ \sqrt{s} \end{pmatrix}, \quad P_B = \frac{1}{2}\begin{pmatrix} \sqrt{s} \\ 0 \\ 0 \\ -\sqrt{s} \end{pmatrix}, \quad q = \begin{pmatrix} Q_0 \\ Q_T \\ 0 \\ Q_z \end{pmatrix}, \tag{3}$$

where $Q_T = \sqrt{\vec{q}_T^{\,2}} = \sqrt{Q_x^2 + Q_y^2}$.
Defining $Q := \sqrt{q^2}$, we get:

$$Q^2 = Q_0^2 - Q_z^2 - Q_T^2. \tag{4}$$

Hadron-level Mandelstam variables are:

$$\begin{aligned} s &= (P_1 + P_2)^2, \\ t &= (q - P_1)^2, \\ u &= (q - P_2)^2. \end{aligned} \tag{5}$$

1.1.2 Dilepton center-of-mass system

Now, we need to specify the axes in the dilepton c.m.s. There are a number of popular axis choices, but we choose so-called the Collins-Soper (CS) frame [4] (Figure 2).

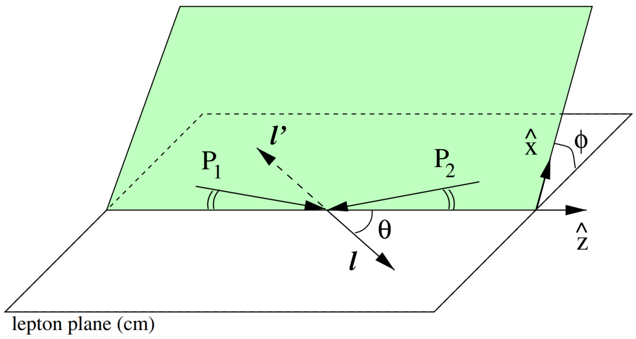

Figure 2: The Collins-Soper frame

The reason of this choice is that the CS frame produces the simplest expressions for the helicity structure functions.

1.2 Cross section

Due to the usage of dilepton c.m.s. frame hadronic and leptonic degrees of freedom are completely factorized [3]. This fact allow us to write differential cross section in following form:

$$d\sigma \sim W^{\mu\nu} L_{\mu\nu}, \tag{6}$$

where $W^{\mu\nu}$ — hadroinc tensor (Figure 3),
$L_{\mu\nu}$ — leptonic tensor (Figure 4).

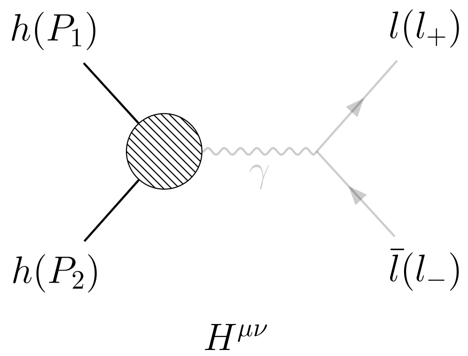

Figure 3: Graphical illustration of hadronic tensor

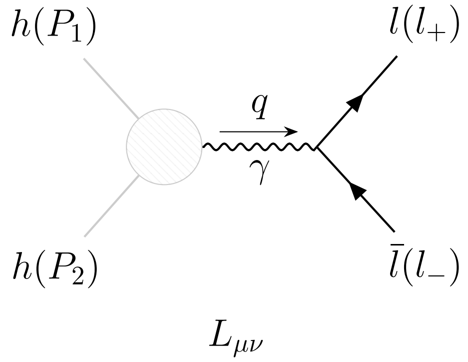

Figure 4: Graphical illustration of leptonic tensor

And we can immediately express leptonic tensor in terms of dilepton pair momenta:

$$L^{\mu\nu} = \mathrm{Tr}\,[\gamma^\mu \not{l}_+ \gamma^\nu \not{l}_-] = 4\bigg(l_-^\mu l_+^\nu - \frac{Q^2}{2} g^{\mu\nu} + l_+^\mu l_-^\nu \bigg). \tag{7}$$

1.3 Helicity structure functions

The Lorentz tensor $W^{\mu\nu}$ can be written as a sum of products of tensors and scalar functions called helicity structure functions:

$$\begin{aligned} W^{\mu\nu} = {} & (X^\mu X^\nu + Y^\mu Y^\nu) W_T + i(X^\mu Y^\nu - X^\nu Y^\mu) W_{T_P} + Z^\mu Z^\nu W_L + \\ & + (Y^\mu Y^\nu - X^\mu X^\nu) W_{\Delta\Delta} - (X^\nu Y^\mu + X^\mu Y^\nu) W_{\Delta\Delta_P} - \\ & - (X^\nu Z^\mu + X^\mu Z^\nu) W_\Delta - (Y^\nu Z^\mu + Y^\mu Z^\nu) W_{\Delta_P} + \\ & + i(X^\nu Z^\mu - X^\mu Z^\nu) W_\nabla + i(Y^\mu Z^\nu - Y^\nu Z^\mu) W_{\nabla_P}, \end{aligned} \tag{8}$$

Lorentz tensors above are orthogonal unit vectors in CM frame, which defined as follows:

$$T^\mu = \frac{q^\mu}{Q}, \tag{9}$$

$$X^\mu = -\bigg(\frac{Q}{Q_T}\bigg) \frac{2}{\sqrt{Q^2 + Q_T^2}} \bigg[\frac{P_2 \cdot q}{\sqrt{s}} \bigg(P_1^\mu - \frac{P_1 \cdot q}{q^2} q^\mu \bigg) + \frac{P_1 \cdot q}{\sqrt{s}} \bigg(P_2^\mu - \frac{P_2 \cdot q}{q^2} q^\mu \bigg) \bigg], \tag{10}$$

$$Z^\mu = \frac{2}{\sqrt{Q^2 + Q_T^2}} \bigg[\frac{P_2 \cdot q}{\sqrt{s}} \bigg(P_1^\mu - \frac{P_1 \cdot q}{q^2} q^\mu \bigg) - \frac{P_1 \cdot q}{\sqrt{s}} \bigg(P_2^\mu - \frac{P_2 \cdot q}{q^2} q^\mu \bigg) \bigg], \tag{11}$$

$$Y^\mu = \epsilon^{\mu\nu\alpha\beta} T_\nu Z_\alpha X_\beta. \tag{12}$$

2 QCD corrections to polarized Drell-Yan process

2.1 Hadronic tensor

First of all, we introduce parton-level Mandelstam variables:

$$\begin{aligned}\hat{s} &= (\xi_1 P_1 + \xi_2 P_2)^2 = \xi_1 \xi_2 s,\\ \hat{t} &= (q - \xi_1 P_1)^2,\\ \hat{u} &= (q - \xi_2 P_2)^2.\end{aligned} \tag{13}$$

We consider the Drell–Yang process as the sum of all possible processes at the parton level in which a dilepton pair can arise:

$$i\mathcal{M} = i\sum_k \mathcal{M}_k\big(h(1)h(2) \to l\bar{l} + X\big), \tag{14}$$

where k is the corresponded matrix element number.

And the transition amplitude in general form can be written as:

$$\left|\hat{\mathcal{M}}\right|^2 = \sum_k \left|\hat{\mathcal{M}}_k\right|^2 + \sum_{a<b} 2\,\mathrm{Re}\left(\hat{\mathcal{M}}_a \hat{\mathcal{M}}_b^*\right) \tag{15}$$

At the leading order of α_s we can distinguish two subprocesses of Drell-Yan process: real emission (Figure 5) and compton-like (Figure 6) process.

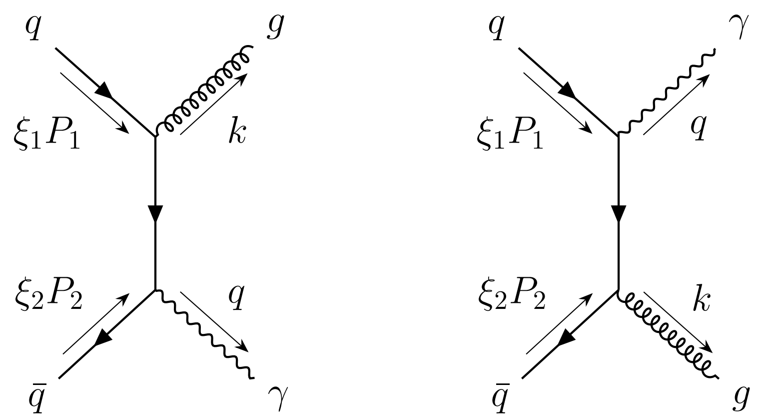

Figure 5: The real emission process

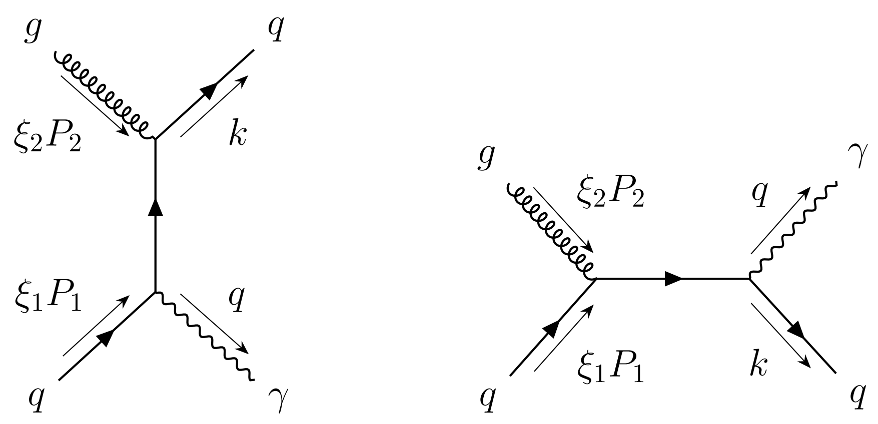

Figure 6: The compton-like process

Due to the fact that we consider polarized partons case of Drell-Yan process, we use quark helicity projection operator:

$$P_{\pm}(p) = \frac{1}{2}\not{p}(1 \pm \gamma_5) \tag{16}$$

and gluon helicity projection operator:

$$P_{\pm}^{\alpha\beta} = \frac{1}{2}\big(d^{\alpha\beta} \pm i\epsilon^{\alpha\beta}\big), \tag{17}$$

where $d^{\alpha\beta} = -g^{\alpha\beta} + \bar{n}^{\alpha}n^{\beta} + n^{\alpha}\bar{n}^{\beta}$ — transverse tensor;
$\epsilon^{\alpha\beta} = \epsilon^{\alpha\beta\rho\sigma}\bar{n}_{\rho}n_{\sigma}$ — antisymmetric part,
n and $\bar{n}$ — are unit vectors in light-cone frame.

Hence, there is appearing antisymmetric part of hadronic tensor. So, it is convenient to divide hadronic tensor into three parts as follows:

$$W_{\mu\nu} = W_{\mu\nu}^{\text{unpol}} + \Delta W_{\mu\nu}^{\text{pol}} + \Delta W_{\mu\nu}^{\text{Asym(pol)}} \tag{18}$$

2.2 Helicity structure functions calculation

As we noted in (Sec. 2.1) there are two subprocesses of Drell-Yan process and for both of them three cases whose are corresponded to unpolarized part, polarized symmetric part and polarized antisymmetric part of hadronic tensor. Therefore, there are six cases for helicity structure functions. Let us consider them consistently.

The main idea is the same for all considering cases. Foremost, we introduce new kinematics variables to simplify our result:

$$\rho = \frac{Q_T}{Q}, \tag{19}$$

$$x_1 = \frac{Q}{\sqrt{s}} e^{y}, \tag{20}$$

$$x_2 = \frac{Q}{\sqrt{s}} e^{-y}, \tag{21}$$

and

$$z_1 = \frac{x_1}{\xi_1}, \qquad z_2 = \frac{x_2}{\xi_2}, \tag{22}$$

where $y = \frac{1}{2}\ln\left(\frac{Q_0 - Q_T}{Q_0 + Q_T}\right)$ —rapidity of boost along z-axis.
After hadronic tensor calculation of corresponded Drell-Yan subprocess by formula (15), we separate Lorentz-structures as it have done in formula (8) and make a comparison with it. Due to this approach, we straightforwardly get expressions of helicity structure functions.

2.2.1 Real emission process

2.2.1.1 Unpolarized part

For unpolarized part of real emission subprocess, we get:

$$w^{\text{unpol}}_{T_P;RE} = w^{\text{unpol}}_{\Delta\Delta_P;RE} = w^{\text{unpol}}_{\Delta_P;RE} = w^{\text{unpol}}_{\nabla;RE} = w^{\text{unpol}}_{\nabla_P;RE} = 0, \tag{23}$$

$$w^{\text{unpol}}_{T;RE} = \frac{16\pi^2 e^2 Q_f^2 \alpha_s \left(z_1^2 + z_2^2\right)}{9 z_1 z_2}\left[\frac{2}{\rho^2} + 1\right] s\delta\big(\hat{s} + \hat{t} + \hat{u} - Q^2\big), \tag{24}$$

$$w^{\text{unpol}}_{L;RE} = \frac{32\pi^2 e^2 Q_f^2 \alpha_s}{9}\frac{z_1^2 + z_2^2}{z_1 z_2} s\delta\big(\hat{s} + \hat{t} + \hat{u} - Q^2\big), \tag{25}$$

$$w^{\text{unpol}}_{\Delta\Delta;RE} = \frac{16\pi^2 e^2 Q_f^2 \alpha_s}{9}\frac{z_1^2 + z_2^2}{z_1 z_2} s\delta\big(\hat{s} + \hat{t} + \hat{u} - Q^2\big), \tag{26}$$

$$w^{\text{unpol}}_{\Delta;RE} = \frac{32\pi^2 e^2 Q_f^2 \alpha_s}{9}\frac{1}{\rho}\frac{z_1^2 - z_2^2}{z_1 z_2} s\delta\big(\hat{s} + \hat{t} + \hat{u} - Q^2\big). \tag{27}$$

2.2.1.2 Polarized part (Symmetric)

For polarized symmetric part of real emission subprocess, we get helicity structure functions which are completely the same as in unpolarized part:

$$\Delta w^{\text{pol}}_{T_P;RE} = \Delta w^{\text{pol}}_{\Delta\Delta_P;RE} = \Delta w^{\text{pol}}_{\Delta_P;RE} = \Delta w^{\text{pol}}_{\nabla;RE} = \Delta w^{\text{pol}}_{\nabla_P;RE} = 0, \tag{28}$$

$$\begin{aligned} &\Delta w^{\text{pol}}_{T;RE} = w^{\text{unpol}}_{T;RE}, \quad \Delta w^{\text{pol}}_{L;RE} = w^{\text{unpol}}_{L;RE}, \\ &\Delta w^{\text{pol}}_{\Delta\Delta;RE} = w^{\text{unpol}}_{\Delta\Delta;RE}, \quad \Delta w^{\text{pol}}_{\Delta;RE} = w^{\text{unpol}}_{\Delta;RE} \end{aligned} \tag{29}$$

2.2.1.3 Polarized part (Antisymmetric)

And for polarized antisymmetric part of real emission subprocess, we get:

$$\begin{aligned} w^{\text{Asym(pol)}}_{T;RE} &= w^{\text{Asym(pol)}}_{L;RE} = w^{\text{Asym(pol)}}_{\Delta\Delta;RE} = w^{\text{Asym(pol)}}_{\Delta\Delta_P;RE} = w^{\text{Asym(pol)}}_{\Delta;RE} = \\ &= w^{\text{Asym(pol)}}_{\Delta_P;RE} = w^{\text{Asym(pol)}}_{\nabla;RE} = 0, \end{aligned} \tag{30}$$

$$w^{\text{Asym(pol)}}_{T_P;RE} = -\frac{64\pi^2 e^2 Q_f^2 \alpha_s}{9} \frac{1}{\rho^2} \sqrt{1+\rho^2} \frac{z_1^2 + z_2^2}{z_1 z_2} s\delta\big(\hat{s} + \hat{t} + \hat{u} - Q^2\big), \tag{31}$$

$$w^{\text{Asym(pol)}}_{\nabla_P;RE} = \frac{64\pi^2 e^2 Q_f^2 \alpha_s}{9} \frac{1}{\rho} \sqrt{1+\rho^2} \frac{z_2^2 - z_1^2}{z_1 z_2} s\delta\big(\hat{s} + \hat{t} + \hat{u} - Q^2\big). \tag{32}$$

We could conclude that taking into account antisymmetric part of hadronic tensor leads us to appearing of two additional helicity structure functions: W_{T_P} and W_{∇_P}.

2.2.2 Compton process

2.2.2.1 Unpolarized part

For unpolarized part of compton-like subprocess we, get:

$$w^{\text{unpol}}_{T_P;CP} = w^{\text{unpol}}_{\Delta\Delta_P;CP} = w^{\text{unpol}}_{\Delta_P;CP} = w^{\text{unpol}}_{\nabla;CP} = w^{\text{unpol}}_{\nabla_P;CP} = 0, \tag{33}$$

$$w^{\text{unpol}}_{T;q(pol)g(pol)} = \frac{2\pi^2 e^2 Q_f^2 \alpha_s}{3}\left[\frac{1}{\rho^2}\frac{2\left(1-z_2\right)\left(z_1^2+\left(z_2-3\right)z_1+\left(2z_2-3\right)z_2+3\right)}{z_1 z_2}-\right.$$
$$\left. -\frac{\left(z_2-1\right)\left(\left(z_1+z_2\right)^2-6z_1+\left(z_2-6\right)z_2+6\right)}{z_1 z_2}\right] s\delta\left(\hat{s}+\hat{t}+\hat{u}-Q^2\right), \tag{34}$$

$$w^{\text{unpol}}_{L;q(pol)g(pol)} = -\frac{4\pi^2 e^2 Q_f^2 \alpha_s \left(z_2-1\right)\left(z_1^2+2z_2 z_1+2z_2^2\right)}{3z_1 z_2} s\delta\left(\hat{s}+\hat{t}+\hat{u}-Q^2\right), \tag{35}$$

$$w^{\text{unpol}}_{\Delta\Delta;q(pol)g(pol)} = -\frac{2\pi^2 e^2 Q_f^2 \alpha_s \left(z_2-1\right)\left(z_1^2+2z_2 z_1+2z_2^2\right)}{3z_1 z_2} s\delta\left(\hat{s}+\hat{t}+\hat{u}-Q^2\right), \tag{36}$$

$$w^{\text{unpol}}_{\Delta;q(pol)g(pol)} = -\frac{4\pi^2 e^2 Q_f^2 \alpha_s}{3}\frac{1}{\rho}\frac{\left(z_2-1\right)\left(z_1^2-2z_2^2\right)}{z_1 z_2} s\delta\left(\hat{s}+\hat{t}+\hat{u}-Q^2\right). \tag{37}$$

2.2.2.2 Polarized part (Symmetric)

For polarized symmetric part of compton-like subprocess, we get:

$$w^{\text{pol}}_{T_P;CP} = w^{\text{pol}}_{\Delta\Delta_P;CP} = w^{\text{pol}}_{\Delta_P;CP} = w^{\text{pol}}_{\nabla;CP} = w^{\text{pol}}_{\nabla_P;CP} = 0, \tag{38}$$

$$\Delta w^{\text{Asym(pol)}}_{T;CP} = \frac{2\pi^2 e^2 Q_f^2 \alpha_s}{3}\left[\frac{1}{\rho^2}\frac{\left(z_1-3\right)\left(z_2-1\right)\left(z_1+2z_2-2\right)}{z_1 z_2}+\right.$$
$$\left. +\frac{z_1^2+\left(z_1-3\right)\left(z_1+2z_2-2\right)\left(z_2-1\right)}{z_1 z_2}\right] s\delta\left(\hat{s}+\hat{t}+\hat{u}-Q^2\right), \tag{39}$$

$$\Delta w^{\text{Asym(pol)}}_{L;CP} = \frac{4\pi^2 e^2 Q_f^2 \alpha_s}{3}\frac{z_1\left(z_2-1\right)\left(z_1+2z_2\right)}{z_1 z_2} s\delta\left(\hat{s}+\hat{t}+\hat{u}-Q^2\right), \tag{40}$$

$$\Delta w^{\text{pol}}_{\Delta\Delta;CP} = \frac{2\pi^2 e^2 Q_f^2 \alpha_s}{3}\frac{z_1\left(z_2-1\right)\left(z_1+2z_2\right)}{z_1 z_2} s\delta\left(\hat{s}+\hat{t}+\hat{u}-Q^2\right), \tag{41}$$

$$\Delta w^{\text{pol}}_{\Delta;CP} = \frac{4\pi^2 e^2 Q_f^2 \alpha_s}{3}\frac{1}{\rho}\frac{z_1^2\left(z_2-1\right)}{z_1 z_2} s\delta\left(\hat{s}+\hat{t}+\hat{u}-Q^2\right). \tag{42}$$

Unlikely to real emission, in the compton-like subprocess helicity structure functions corresponded to unpolarized and polarized symmetric cases are different.

2.2.2.3 Polarized part (Antisymmetric)

And for polarized antisymmetric part of compton-like subprocess, we get:

$$
\begin{aligned}
w_{T;CP}^{\text{Asym(pol)}} &= w_{L;CP}^{\text{Asym(pol)}} = w_{\Delta\Delta;CP}^{\text{Asym(pol)}} = w_{\Delta\Delta_P;CP}^{\text{Asym(pol)}} = w_{\Delta;CP}^{\text{Asym(pol)}} = \\
&= w_{\Delta_P;CP}^{\text{Asym(pol)}} = w_{\nabla;CP}^{\text{Asym(pol)}} = 0,
\end{aligned} \tag{43}
$$

$$
w_{T_P;CP}^{\text{Asym(pol)}} = \frac{8\pi^2 e^2 Q_f^2 \alpha_s}{3} \frac{1}{\rho^2} \sqrt{1+\rho^2} \frac{z_2^2(z_2-1)}{z_1 z_2} s\delta\big(\hat{s}+\hat{t}+\hat{u}-Q^2\big), \tag{44}
$$

$$
w_{\nabla_P;CP}^{\text{Asym(pol)}} = -\frac{8\pi^2 e^2 Q_f^2 \alpha_s}{3} \frac{1}{\rho} \sqrt{1+\rho^2} \frac{z_2^2(z_2-1)}{z_1 z_2} s\delta\big(\hat{s}+\hat{t}+\hat{u}-Q^2\big). \tag{45}
$$

Similarly, as in the real emission case, we have two additional helicity structure functions.

CONCLUSION

This work provided a theoretical analysis of the Drell-Yan process, including considerations of the kinematics in the center-of-mass systems of hadrons and dileptons, factorization of the scattering cross-section into leptonic and hadronic tensors, and parameterization of the hadronic tensor. Feynman diagrams corresponding to the first-order QCD corrections to the Drell-Yan process were constructed and compared with the corresponding matrix elements.

As a result, analytical expressions for the helicity structure functions of the polarized Drell-Yan process at the first order of the strong coupling constant were obtained. It was found that the polarization of partons leads to the emergence of two additional helicity structure functions W_{T_P} and W_{∇_P} compared to the unpolarized case.

Furthermore, it is of interest to explore, in addition to the Z boson and W bosons, the kinematic region $\rho \to 0$.

REFERENCES

1. Boer D. Drell–Yan lepton angular distribution at small transverse momentum / D. Boer, W. Vogelsang // Physical Review D. – 2006. Vol. 74, – ISSN 2470-0010.

2. Drell S. D. Massive lepton pair production in hadron–hadron collisions at high–energies / S. D. Drell, Toung-Mow Yan, // Physical Review Letters – 1970. Vol. 25, – ISSN 1079-7114.

3. Rodriguez-Pedraza R.A. QCD resummation for the fully differential Drell–Yan cross section : dis. ...doctor of philosophy / R.A. Rodriguez-Pedraza – Iowa, 2007. – 150 p.

4. Lam C. S. Systematic approach to inclusive lepton pair production in hadronic collisions / C. S. Lam, Wu-Ki Tung, // Physical Review D. – 1978. Vol. 18, – ISSN 2470-0010.

5. Berger E. L. Transverse momentum dependence of the angular distribution of the Drell–Yan process / E. L. Berger, Jian-Wei Qiu, R. A. Rodriguez-Pedraza // Physical Review D. – 2007. Vol. 76, – ISSN 2470-0010.